APPLIED ORGANOMETALLIC CHEMISTRY
Appl. Organometal. Chem. 2005; **19**: 1047–1054
Published online in Wiley InterScience (www.interscience.wiley.com). DOI:10.1002/aoc.956

Synthesis of Ti-MCM-41 directly from silatrane and titanium glycolate and its catalytic activity[1]

N. Thanabodeekij[1], W. Tanglumlert[1], E. Gulari[2] and S. Wongkasemjit[1]*

[1]The Petroleum and Petrochemical College, Chulalongkorn University, Bangkok 10330, Thailand
[2]Department of Chemical Engineering, University of Michigan, Ann Arbor, MI 48109-2136, USA

Received 1 April 2005; Revised 19 May 2005; Accepted 31 May 2005

Titanium is successfully incorporated in hexagonal mesoporous silica to form Ti-MCM41 at low temperature. Silatrane and titanium glycolate synthesized from the oxide one-pot synthesis process are used as the precursors. Using the cationic surfactant cetyltrimethylammonium bromide as a template, the resulting meso-structure mimics the liquid-crystal phase. The percentage of titanium loading is varied in the range 1–35%. The temperatures used in the preparation are 60 °C and 80 °C. After heat treatment, very high surface area mesoporous silica was obtained and characterized using diffuse reflectance UV (DRUV) spectroscopy, X-ray diffraction (XRD), BET surface area, X-ray fluorescence, energy dispersive spectroscopy and transmission electron microscopy (TEM). At 35% titanium, the titanium atom is also in the framework showing the pattern of hexagonal mesostructure, as shown by DRUV, XRD and TEM results. The surface area is extraordinarily high, up to more than 2300 $m^2 g^{-1}$, and the pore volume is as high as 1.3 $cm^3 g^{-1}$ for a titanium loading range of 1–5%. Oxidative bromination reaction using Ti-MCM-41 as catalyst showed impressive results, with the 60 °C catalysts having higher activity. Copyright © 2005 John Wiley & Sons, Ltd.

KEYWORDS: silatranes; titanium glycolate; mesoporous silica; CTAB; sol–gel process

INTRODUCTION

Catalytic oxidation is an important process in the production of fine chemicals. It was discovered that TS-1 and its extension as TS-β and TS-ZSM are active for selective oxidation of various compounds in the presence of hydrogen peroxide.[1] However, large organic molecules cannot access the active sites located inside the small cavities and channels of the zeolite. The M41S family of larger pore zeolites was discovered by Mobil researchers. The new materials, designated as mesoporous molecular sieves (MMSs), include hexagonal MCM-41, cubic MCM-48 and lamellar MCM-50 phases.[2] The preparation of the M41S family involves liquid-crystal formation by the cationic surfactant cetyltrimethylammonium bromide (CTAB).[3–5] The high surface area (over 1000 $m^2 g^{-1}$), the monodisperse pore sizes in the range of 2–50 nm, and a high degree of stereoregularity mimicking the liquid-crystal structure used in their preparation result in a catalyst with almost no mass transfer limitation. In addition, titanium supported on MMSs showed a promising oxidation reaction of large organic molecules with hydrogen peroxide as the oxidizing agent, and it could also be used as a photocatalyst.

Titanium-incorporated MCM-41 was prepared by either grafting titanium precursor on to surface silanols via a post-synthetic procedure or depositing titanium precursor on MCM-41 from the sol obtained by controlled hydrolysis of a titanium alkoxide precursor followed by calcination. In this paper, metal alkoxide precursors, namely silatrane and titanium glycolate, were used for producing mesostructure materials because of their moisture stability, resulting in the ability to control hydrolysis and condensation. The precursors were synthesized directly from inexpensive metal oxide SiO_2 and TiO_2 via the oxide one-pot synthesis (OOPS) process. This process gave high-purity metal alkoxide products, having been successfully used for syntheses

*Correspondence to: S. Wongkasemjit, The Petroleum and Petrochemical College, Chulalongkorn University, Bangkok 10330, Thailand.
E-mail: dsujitra@chula.ac.th
Contract/grant sponsor: Postgraduate Education and Research Program in Petroleum and Petrochemical Technology (ADB) Fund.
Contract/grant sponsor: Ratchadapisake Sompote Fund.
Contract/grant sponsor: Chulalongkorn University.
Contract/grant sponsor: Thailand Research Fund.

of high-quality microporous zeolites, such as LTA,[6] ANA and GIS,[7] and MFI.[8] In general, the most active and selective sites of titanium-supported heterogeneous catalysts are isolated, mononuclear, 4-coordinated titanium(IV) centers.

It has been recognized that the most promising oxidation catalyst is the catalyst containing isolated active sites, meaning one or only a few metal incorporated centers on the surface of an oxide support. Typically, these active sites are associated with a specific inorganic structure, giving rise to the desired catalytic properties. Thus, the highlight of this paper is the preparation of high-percentage loadings of titanium-incorporated MCM-41 with high surface area while maintaining the MCM-41 hexagonal structure, to provide the highest concentration of active sites per unit volume of catalyst.

EXPERIMENTAL

Materials

Fumed silica (SiO_2) was purchased from Aldrich Chemical Co. Titanium dioxide, potassium bromide (KBr) and hydrogen peroxide (H_2O_2) were purchased from Carlo Erba. 2-[(4-Hydroxyphenyl)(4-oxo-2,5-cyclohexadien-1-ylidene)methyl]benzene sulfonic acid (phenol red), ethylene glycol ($HOCH_2CH_2OH$) and triethanolamine (TEA, $N(CH_2CH_2OH)_3$) were supplied by Labscan Asia Co., and used as received. Acetonitrile was also obtained from Labscan Asia Co. and distilled before use. CTAB and sodium hydroxide were purchased from Sigma Chemical Co. HEPES buffer solution (4-(2-hydroxyethyl)-1-piperazineethanesulfonic acid) was obtained from Fluka.

Material characterization

Mass spectra of precursors were obtained on a FISONS Instruments 707 VG Autospec-ultima mass spectrometer (Manchester, UK) with VG data system, using the positive fast atom bombardment (FAB^+) mode. Fourier transform IR (FTIR) spectroscopic analysis was conducted using a Bruker Instrument (EQUINOX55) with a resolution of 4 cm^{-1}. The solid sample was prepared by mixing 1% of sample with anhydrous KBr. Thermal properties were analyzed using a Du Pont Instrument TGA 2950 thermogravimetric analyzer.

The mesoporous product was characterized using a Rigaku X-ray diffractometer with Cu Kα source at a scanning speed of 0.75° s^{-1}. The working range was $2\theta = 1.5–10°$. An electron microscope study (transmission electron microscopy (TEM) micrographs and electron diffraction patterns) were carried out using a JEOL 2010F instrument. Surface area and average pore size were determined by the BET method using a Quantasorb Jr. (Autosorb-1). The product was degassed at 250 °C for 12 h prior to analysis. Diffuse reflectance UV (DRUV) spectroscopy was used to identify the location and the coordination of titanium in the hexagonal structure. The reflectance output from the instrument was converted using the Kubelka–Munk algorithm. The titanium content was characterized using scanning electron microscopy (SEM)/energy dispersive spectroscopy (EDS) and X-ray fluorescence (XRF). The calcination was conducted using a Carbolite Furnace (CFS 1200) with a heating rate of 1 °C min^{-1}.

Silatrane synthesis

Wongkasemjit and coworkers' synthetic method[9,10] was followed by mixing silicon dioxide (0.10 mol, 6 g), and TEA (0.125 mol, 18.6 g) in a simple distillation set using 100 ml ethylene glycol solvent. The reaction was done at the boiling point of ethylene glycol under nitrogen atmosphere to remove water as a by-product along with ethylene glycol from the system. The reaction was run for 10 h and excess ethylene glycol was removed under vacuum (1.6 Pa) at 110 °C. The brownish white solid was washed with dried acetonitrile three times. The white powder product was characterized using FTIR spectroscopy, thermogravimetric analysis (TGA) and FAB^+ mass spectrometry (MS).

FTIR bands observed were: 3000–3700 cm^{-1} (w, intermolecular hydrogen bonding of O–H), 2860–2986 cm^{-1} (s, ν_{C-H}), 1244–1275 cm^{-1} (m, ν_{C-N}), 1170–1117 (bs, ν_{Si-O}), 1093 (s, ν_{Si-O-C}), 1073 (s, ν_{C-O}), 1049 (s, ν_{Si-O}), 1021 (s, $\nu_{C-}O$), 785 and 729 (s, ν_{Si-O-C}) and 579 cm^{-1} (w, Si ← N). TGA showed one sharp mass loss transition at 390 °C and gave 18.5% ceramic yield, corresponding to $Si((OCH_2CH_2)_3N)_2H_2$. FAB^+-MS showed the highest m/e at 669 of $Si_3((OCH_2CH_2)_3N)_4H^+$ and 100% intensity at 323 of $Si((OCH_2CH_2)_3N)_2H^+$.

Titanium glycolate synthesis

A mixture of titanium dioxide (0.025 mol, 2 g), triethylenetetramine (0.007 mol, 3.7 g), used as a catalyst, and 25 ml of ethylene glycol, used as a solvent, was heated to the boiling point of ethylene glycol for 24 h, followed by separating the unreacted TiO_2 from the solution part. The excess ethylene glycol and triethylenetetramine were removed by vacuum distillation to obtain the crude white solid product. The crude product was then washed with acetonitrile and dried in a vacuum desiccator before characterization using FTIR spectroscopy, TGA, and FAB^+-MS.[11]

FTIR bands observed were: 3000–3700 cm^{-1} (w, trace of water absorbed in the product), 2860–2986 cm^{-1} (s, ν_{C-H}), 1244–1275 cm^{-1} (m, ν_{C-N}), 1170–1117 (bs, ν_{Si-O}), 1093 (s, ν_{Si-O-C}), 1073 (s, ν_{C-O}), 1049 (s, ν_{Si-O}), 1021 (s, ν_{C-O}), 785 and 729 (s, ν_{Si-O-C}) and 579 cm^{-1} (w, Si ← N). The TGA result showed one sharp mass loss corresponding to the decomposition of organic ligand and remaining organic residue around 310–350 °C and gave 46.8% ceramic yield, which is close to the theoretical yield

of 47.5%. FAB^+-MS showed m/e 169 with 8.5% intensity of $Ti(OCH_2CH_2O)_2$.

Synthesis of Ti-MCM-41

Various ratios of silatrane and titanium glycolate precursors in the range 1–35% titanium were studied by adding into a solution containing 112×10^{-5} mol CTAB, 1×10^{-3} mol NaOH and 14×10^{-3} mol TEA. 36×10^{-2} mol of water was then added with vigorous stirring at 60 °C and 80 °C. The mixture was stirred for various times to follow the reaction using DRUV spectroscopy. The crude product obtained was filtered and washed with water to obtain a white solid. The white solid was dried at room temperature and calcined at 550 °C for 3 h to obtain mesoporous Ti-MCM-41, which was characterized using X-ray diffraction (XRD), XRF, EDS, BET surface area and TEM.

Catalytic activity study

The peroxidative bromination test was used to study catalyst activity qualitatively. Ti-MCM-41 was added into a mixture of 0.2 mM phenol red, 0.1 M KBr, 10 mM H_2O_2 in 0.1 M HEPES buffer having pH 6.5. Then, the mixture was stirred for various times. The total volume of the mixture was 3.5 ml. The formation of 2-[(3,5-dibromo-4-hydroxyphenyl)(3,5-dibromo-4-oxo-2,5-cyclohexadien-ylidene)methyl]benzenesulfonic acid (bromophenol blue) from phenol red was monitored by UV–vis after removing the solid catalyst.

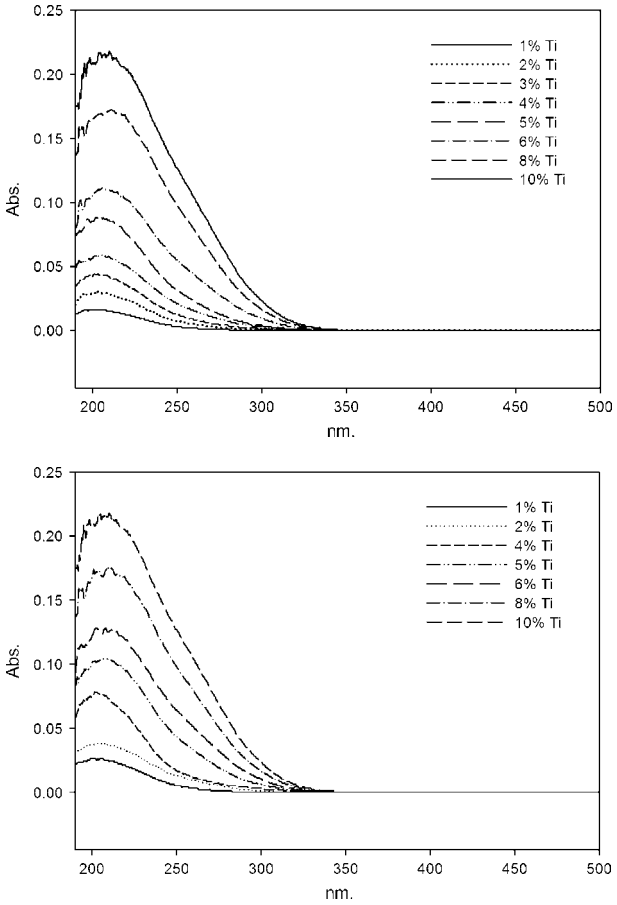

Figure 1. DRUV spectra of Ti-MCM-41 containing titanium loadings of 1–10% at (a) 60 °C and (b) 80 °C.

RESULTS AND DISCUSSION

Ti-MCM41 characterization

DRUV spectroscopy was used to determine the site of titanium and to determine the presence of extra-framework titanium in our synthesized Ti-MCM41. In general, the DRUV absorbance pattern depends on the titanium content, synthesis procedure used and site where titanium is incorporated.[12–15] For small amounts of well-dispersed titanium, the DRUV peak will show only an isolated, tetrahedrally coordinated species, as indicated by the peak at $\lambda = 200–230$ nm; see Fig. 1 when the incorporated titanium is not more than 5%. The band can be interpreted as a ligand-to-metal charge-transfer transition from oxygen to isolated tetrahedral titanium(IV).[16,17] When the coordination number is more than four, such as bonding with water molecules beside the metal coordination sphere, the absorption band will be shifted to longer wavelengths or lower energies. In Fig. 1, the 1–10% titanium-incorporated MCM-41 is almost in the form of isolated titanium(IV), referring to the presence of the intense band mainly around 220 nm, for both 60 °C and 80 °C reaction temperatures. However, with increasing titanium content the DRUV band is shifted a little to longer wavenumbers, probably due to ligand-to-metal charge transfer involving isolated titanium atoms in an octahedral environment, from which two water molecules are bonded.[13,14] In fact, it has been reported that materials containing small amounts of well-dispersed titanium (~2%) will generally form isolated tetrahedrally coordinated titanium,[16] and Maschmeyer and coworkers[18] reported that TEA was found to act not only as a template, but also as a director for positioning titanium-sites to form isolated tetrahedrally coordinated titanium species. When the percentage of titanium increased, the DRUV peak was broader and showed a very small shoulder at $\lambda = 280$ nm, as shown in Fig. 2. This peak pattern corresponds to partially polymerized titanium species (five- and six-coordinated).[15,19] The red shift and broad band for mesoporous titanium samples may be an indication that at higher titanium contents there is a higher possibility of titanium forming in either a disordered tetrahedral environment or in octahedral coordination spheres. The DRUV spectrometer is a sensitive instrument for detecting the extra-framework titanium absorption at around 330 nm, but band spectra at 330 nm did not appear in our samples, meaning that extra-framework or clusters of titanium in MCM-41 were not present for all conditions studied. This implies that our synthesized silatrane and titanium glycolate hydrolyze and

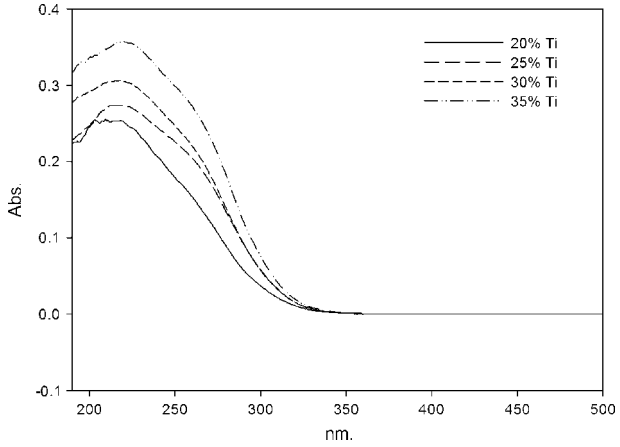

Figure 2. DRUV spectra of Ti-MCM-41 at various titanium loadings.

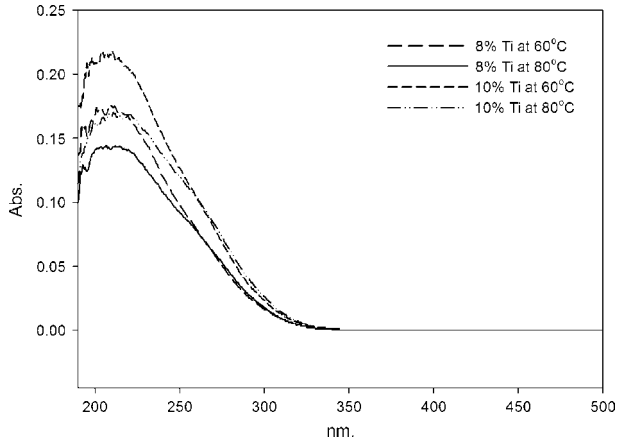

Figure 3. Comparison of DRUV spectra of Ti-MCM-41 at titanium loadings of 8% and 10% at reaction temperatures of 60 and 80 °C.

condense together very well. Amoros and coworkers[3–5,20–21] also synthesized mesoporous oxide using silatrane[22] and titanatrane precursors to form high-percentage titanium-containing mesoporous silica for epoxidation studies. In their work, the minimum silicon/titanium ratio was as low as 1.9.[20] Their success came from the ability to control hydrolysis and condensation processes. Silatrane is quite inert towards hydrolysis compared with other alkoxide precursors; thus, it can be used to introduce highly active tetrahedral-site titanium into mesoporous silica. However, titanatrane was not as inert for hydrolysis as reported by Amoros and coworkers. Titanium glycolate in our work, on the other hand, is much more stable; thus, the synthesis provided a higher percentage of titanium incorporated into MCM-41. Comparing synthesis at 60 °C and 80 °C, the higher temperature gave a broader band and showed a more intense shoulder at $\lambda = 280$ nm (Fig. 3), indicating the presence of higher concentration of partially polymerized titanium species (contain more Ti–O–Ti bonds).[19] This result was probably due to the sensitivity of both silatrane and titanium glycolate precursors towards higher temperature.

The calcined products at various titanium contents showed a well-resolved pattern of a hexagonal mesostructure, as shown in Fig. 4. In this figure, XRD spectra give only (*hk*0) reflections, and no reflections at diffraction angles larger than $2\theta = 6°$ were observed. The positions of these peaks approximately fit with the position for the (*hk*0) reflections of a hexagonal unit cell with $a = b$ and $c = \infty$.[23,24] The three-peak positions of the (100), (110) and (200) reflections are from long-range structural order of hexagonal arrays. However, at high percentages of titanium the XRD patterns showed a less-crystalline material, as indicated by the lower intensity of the (100) reflection peak and the smaller and less isolated (110) and (200) reflection peaks. Nevertheless, when titanium is more than 10% the 3 h synthesis time is not enough for hexagonal arrays to form, as can be seen in the XRD spectrum containing no (110) and (200) reflections. This is in agreement with the reports in Refs 25–27. However, after increasing the synthesis time to 8 h, the (110) and (200) reflections appeared again, due to the larger size of the titanium ions needing more time to diffuse into the lattice sites.[28] Thus, at high titanium contents, longer times are needed for diffusion and condensation into the hexagonal pattern. Increasing the titanium loading up to 35% resulted in the disappearance of the (110) and (200) reflections, as shown in Fig. 5. However, the pattern of MCM-41 still remained. It is the highlight of our work that the pattern of MCM-41 can be retained as high titanium loadings were incorporated. The main reason for this result probably comes from our extraordinary alkoxide precursors, silatrane and titanium glycolate, having highly pure and moisture-stable properties. Ozin and coworkers[29,30] also used glycometallate precursors to prepare hexagonal mesoporous silica: the non-aqueous lamellar phase of the glycometallate precursor changed into hexagonal mesophase when hydrolyzed with water.

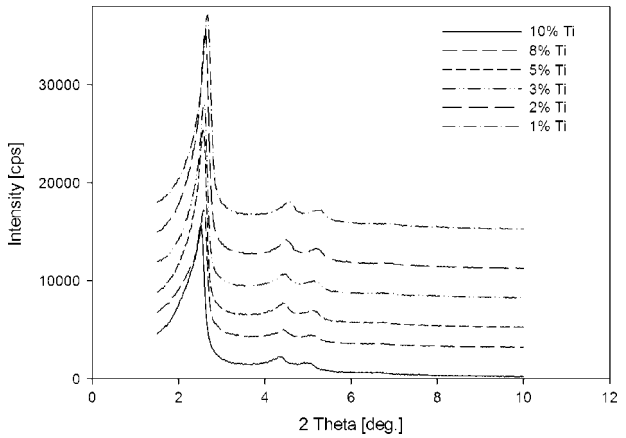

Figure 4. XRD spectra of Ti-MCM-41 containing various titanium loadings.

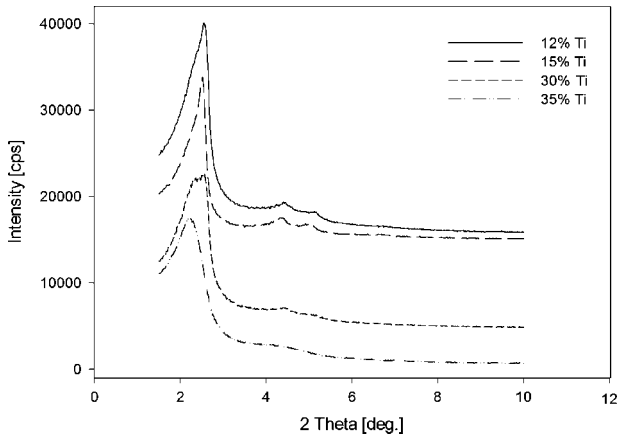

Figure 5. XRD spectra of Ti-MCM-41 at titanium loadings of 12, 15, 30 and 35%.

However, it needed post-treatment with Si_2H_6 to reinforce the meso-structure, due to the collapse of the unstable product structure upon the removal of the surfactant template. The collapsed structure is due to an insufficient degree of silica polymerization arising from structural defects during phase transformation.

FTIR spectra of Ti-MCM-41 are shown in Fig. 6; the absorption peak at 970 cm^{-1} is assigned to the vibrational peak of titanium silicate and considered as the fingerprint of the titanium framework. It was first assigned as a Ti═O group.[25] However, this peak assignment was later discounted and interpreted in terms of Si–OH groups and Ti–O–Si bonds.[25,26] The 950–970 cm^{-1} band is increased in intensity with increasing amount of titanium. This result was explained by the 970 cm^{-1} band being essentially due to the increased degeneracy of the elongation vibration in the tetrahedral structure of SiO_4 induced by the change in the polarity of the Ti–O bonds when silicon is linked to titanium.[25,26] The SiOH groups sharing the OH group with titanium are then responsible for the absorption at higher wavenumbers compared with the unshared Si–OH group.

Nitrogen physisorption probes the textural properties of materials, such as surface area, pore size, pore volume and pore geometry. The nitrogen adsorption–desorption isotherms of pure Ti-MCM-41 at various titanium loadings are shown in Fig. 7. The BET surface area, pore size and pore volume of Ti-MCM-41 are summarized in Table 1. Figure 7 shows that all the isotherms are of the IUPAC type IV classification with five distinct regions. At low relative pressure P/P_0 a very large amount of nitrogen becomes physisorbed in the form of a monolayer on the surface of MCM-41 (both inside and on the external surfaces of the mesopores). Region II is the multilayer adsorption. Region III (Fig. 7a) shows a sharp inflection with relative pressure >0.3, and is characteristic of capillary condensation within uniform pores. Because filling of the mesopores takes

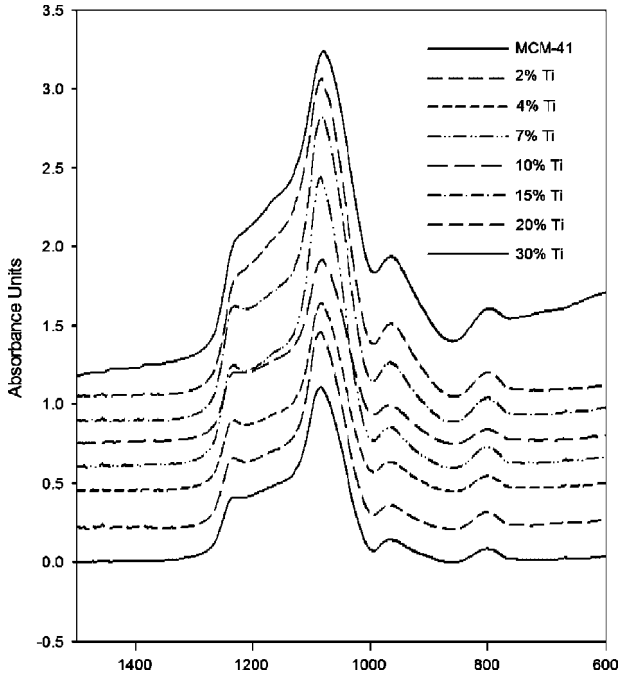

Figure 6. FTIR spectra of Ti-MCM-41 containing various titanium loadings.

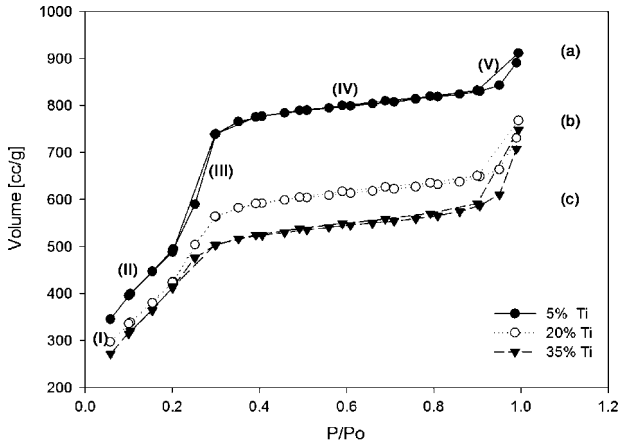

Figure 7. Comparison of nitrogen adsorption isotherms of Ti-MCM-41 at various titanium loadings.

place over a relatively small range of relative pressure, this is indicative of nearly equal-sized pores. Further support for this interpretation is that the desorption curve almost completely coincides with the adsorption isotherm in this pressure range. Surprisingly, Table 1 shows that at higher titanium loadings the pore size is increased. This is contrary to the many papers stating that higher titanium loadings decrease the pore size. However, it was also noted by Bharat *et al.*[26] that an increase in the mesopore size was observed when increasing titanium loadings when using the microwave technique. This result corresponds to a decrease in pore wall thickness of the crystallite sample

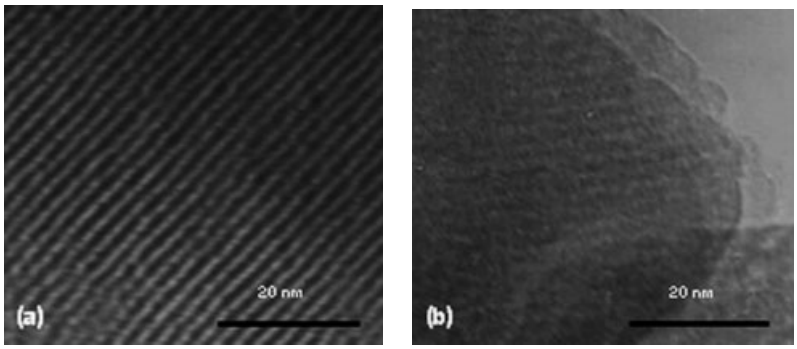

Figure 8. TEM images in perpendicular direction of (a) MCM-41 and (b) 5% titanium-loaded MCM-41 obtained at a reaction temperature of 60 °C.

Table 1. The BET analysis of Ti-MCM-41 synthesized at different titanium loading temperature

Ti (%)	BET surface area ($m^2\ g^{-1}$)	Pore volume ($cm^3\ g^{-1}$)	Average pore size (nm)
60 °C			
1	2351	1.21	2.07
3	2371	1.28	2.11
5	2314	1.38	2.19
15	1827	1.26	2.33
20	1834	1.19	2.58
30	1864	1.23	2.64
35	1707	1.39	2.78
80 °C			
1	2324	1.41	2.33
3	2475	1.61	2.32
5	2417	1.66	2.32
15	1711	1.29	2.55
20	1705	1.26	2.66
30	1724	1.23	2.65
35	1600	1.12	2.81

Table 2. The EDS analysis of Ti-MCM41 synthesized at different titanium loadings and temperature

Temp. (°C)	Ti loading (%)							
	3	5	10	15	20	25	30	35
60	2.96	5.06	10.38	15.6	20.62	24.57	28.68	32.87
80	2.95	5.22	10.64	15.43	20.22	24.85	28.58	33.01

and indicates that the titanium-substituted MCM-41 could be crystallized without decreasing mesopore size via our normal synthesis process. The BET surface areas of our synthesized Ti-MCM-41 are very high compared with others,[25–27] whereas the pore size is comparable. Our previous work has shown that the synthesis of MCM-41 by controlling ion concentration, reaction time, reaction temperature and surfactant concentration results in remarkably high surface area for MCM-41, increasing significantly from 1100 $m^2\ g^{-1}$ to around 2000 $m^2\ g^{-1}$.[31] Again, the main reason comes from the fact that our highly pure and moisture-stable silatrane and titanium glycolate can be manipulated to achieve the balance between hydrolysis and condensation reactions for the extremely high-surface-area MCM-41 synthesis. Amoros and coworkers,[20] who also used silatrane as precursor, obtained a smaller surface area; this was probably due to the difference in precursor synthesis methods giving different silatrane derivatives and, hence, providing different precursor reactivity.

To confirm the XRD results, MCM-41 produced at 60 °C was analyzed using TEM (Fig. 8); the image shows clearly visible cylindrical cross-sections of channels in the perpendicular direction.[24] The periodicity of the pore size calculated from the TEM image is 2.35 nm for unloaded MCM-41 and 2.2 for 5% titanium-loaded MCM-41. The amount of titanium incorporated was determined using both XRF and EDS. The results showed that the titanium incorporation is almost the same as the experimental titanium loading, as summarized in Table 2.

Catalytic activity

Transition-metal ions isomorphously substituted into the tetrahedral framework of micro- and meso-porous molecular sieves have promising catalyst applications. Their activity includes hydroxylation, epoxidation and oxidation reaction. Because of their large surface area and monodispersed pore size, they offer the opportunity to create reaction sites and molecular confinement to permit selective product formation, especially in biocatalytic processes. Peroxidative bromination is successfully catalyzed using vanadium bromoperoxidase (V-BrPO) and hydrogen peroxide as an oxidant under mild conditions.[32] Ti-MCM-41 has been discovered to biomimic the function of vanadium bromoperoxidase at neutral pH.[28,33,34] Phenol red, $\lambda_{max} = 450$ nm, would be transformed into

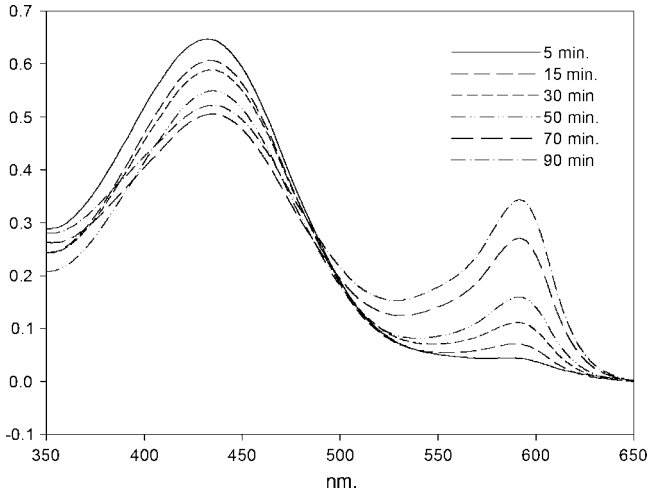

Figure 9. UV–vis absorption spectra of solutions peroxidatively brominated phenolsulfonephthalein (phenol red) catalyzed by Ti-MCM-41, and taken after 5, 15, 30, 50, 70 and 90 min.

bromophenol blue, $\lambda_{max} = 589$ nm,[34] when reacted with only a small amount of Ti-MCM41 catalyst (3–5 mg). The structures of phenol red and bromophenol blue are illustrated in Eqn (1) and the formation of bromophenol blue from phenol red in this work was monitored and shown in Fig. 9.

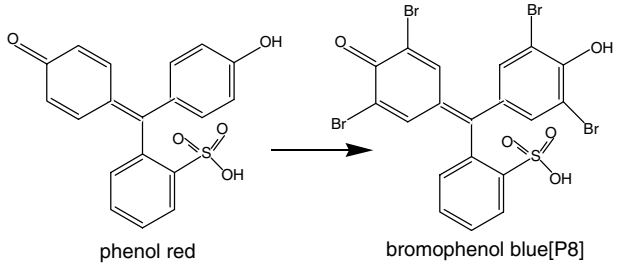

(1)

As shown in Fig. 9, by increasing the reaction time the absorbance at $\lambda_{max} = 589$ nm is increased, indicating the increasing bromination of phenol red to form bromophenol blue with time. It was reported that the function of titanium(IV) is to coordinate and activate H_2O_2 for bromine oxidation represented by an absorbance band at 400 nm. The results are consistent with the formation of peroxotitanium species.[35] Figure 10 shows the plots of the absorbance band at 589 nm for various times and various titanium loadings. Additionally, MCM-41 containing no titanium was also tested for activity: the bromination reaction does not occur, as can be seen in the graph. This evidence was also reported in Ref. 34 when MCM-41 and MCM-48 were studied. If the solution mixture was kept stirred for 56 h, then absorbance at 589 nm was detected. The intensity is comparable with the intensity of the 10% titanium loading detected at 90 min reaction time. The same conditions were studied in the case of TiO_2, where no activity at the time studied was observed.

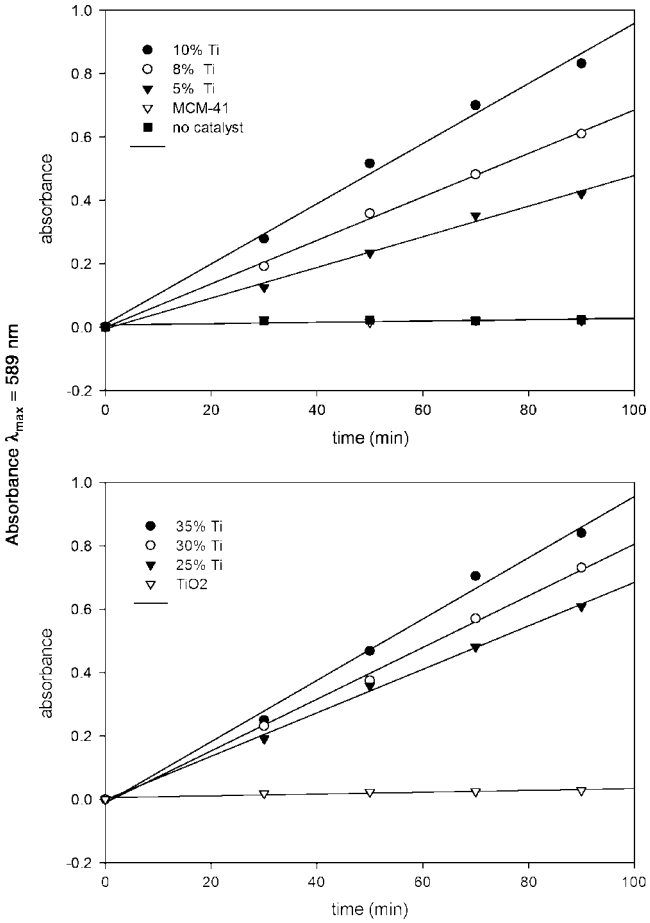

Figure 10. Comparison of the peroxidative bromination reaction at various titanium loadings using (a) 5 mg and (b) 3 mg of catalyst.

However, after continuously stirred for almost 30 h, the solution gradually turned to blue. The absorbance intensity increases when increasing the titanium loading at the same reaction time. Interestingly, the activity kept increasing even at a 35% titanium loading. This result, indeed, indicates no titania cluster formation, which is coincident with the DRUV results. If a cluster of titanium was formed, then it would not be accessible for peroxide coordination, resulting in limited active catalyst.

The effect of the reaction temperature, 60 and 80 °C, is presented in Fig. 11. The activity of catalyst prepared at 60 °C is better, since the presence of a higher absorbance band at $\lambda_{max} = 589$ nm is detected at the same reaction time. The reason comes from more partially polymerized titanium species formed at the reaction temperature of 80 °C, whereas the 60 °C reaction temperature gives more isolated titanium species; this is also confirmed by the previous DRUV results shown in Fig. 3. Moreover, the surface area of solid catalyst prepared at 60 °C is higher; thus, it provides a greater number of active sites per unit volume of catalyst and a higher number of isolated titanium sites.

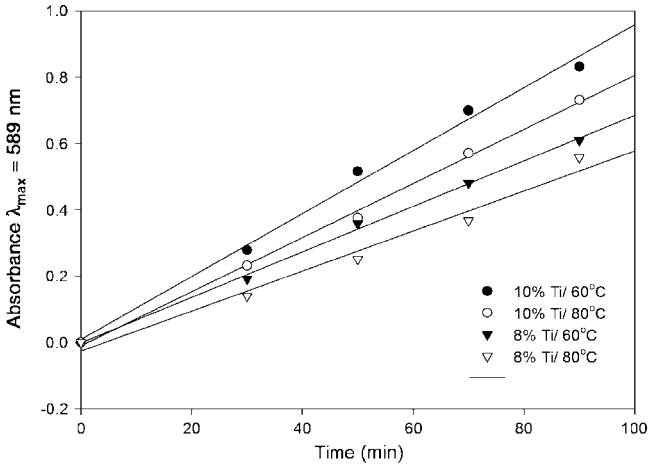

Figure 11. Comparison of catalyst activity of Ti-MCM-41 at titanium loadings of 30 and 35% prepared at reaction temperatures of 60 and 80 °C.

CONCLUSIONS

Silatrane and titanium glycolate precursors synthesized via the OOPS process was successfully used to prepare Ti-MCM-41 catalyst. The structure of MCM-41 is not affected by the increase in titanium loading. The BET surface area was as high as 2300 $m^2 g^{-1}$ for titanium loadings in the range 1–5%. The titanium incorporation is mainly in the form of isolated titanium species when titanium loading is not more than 10%, as probed by DRUV. The hexagonal pore structure was observed using XRD and TEM. The pore sizes are very uniform, as shown by the presence of sharp and clear separation of the (100), (110) and (200) reflections peaks and sharp inflection of the nitrogen adsorption isotherm. The peroxidative bromination test showed good activity of the synthesized catalyst for both catalysts prepared at 60 and 80 °C. However, the activity of catalyst prepared at 60 °C is higher due to the presence of a higher concentration of isolated titanium species.

Acknowledgements

This research work is supported by the Postgraduate Education and Research Program in Petroleum and Petrochemical Technology (ADB) Fund, Ratchadapisake Sompote Fund, Chulalongkorn University and the Thailand Research Fund (TRF).

REFERENCES

1. Phillip ES, Richard AC. *J. Phys. Chem. B* 1999; **103**: 1084.
2. Beck JS, Vartuli JC, Roth WJ, Leonowicz ME, Kresge CT, Schmitt KD, Chu C, Olson DH, Sheppard EW, McCullen SB, Higgins JB, Schlenker JL. *J. Am. Chem. Soc.* 1992; **114**: 10 834.
3. Haskouri JE, Cabrera S, Caldes M, Alamo J, Beltran-Porter A, Marcos MD, Amoros P, Beltran-Porter D. *Int. J. Inorg. Mater.* 2001; **3**: 1157.
4. Haskouri JE, Cabrera S, Caldes M, Alamo J, Beltran-Porter A, Marcos MD, Amoros P, Beltran-Porter D. *Chem. Mater.* 2002; **14**: 2637.
5. Cabrera S, Haskouri JE, Carmen G, Julio L, Beltran-Porter A, Beltran-Porter D, Marcos MD, Amoros P. *Solid State Sci.* 2000; **2**: 405.
6. Sathupanya M, Gulari E, Wongkasemjit S. *J. Eur. Ceram. Soc.* 2002; **22**: 1293.
7. Sathupanya M, Gulari E, Wongkasemjit S. *J. Eur. Ceram. Soc.* 2003; **23**: 2305.
8. Phiriyawirut P, MagarJaphan R, Jamieson AM, Wongkasemjit S. *Mater. Sci. Eng. A* 2003; **361**: 147.
9. Charoenpinijkarn W, Sawankruhasn M, Kesapabutr B, Wongkasemjit S, Jamieson AM. *Eur. Polym. J.* 2001; **37**: 1441.
10. Thitinum S, Thanabodeekij N, Jamieson AM, Wongkasemjit S. *J. Eur. Ceram. Soc.* 2003; **23**: 417.
11. Phonthammachai N, Chairassameewong T, Gulari E, Jamieson AM, Wongkasemjit S. *J. Met. Mater. Min.* 2003; **12**: 23.
12. Marchese L, Maschmeyer T, Gionotti E, Dellarocca V, Rey F, Coluccia S, Thomas JM. *Phys. Chem. Chem. Phys.* 1999; **1**: 585.
13. Ettireddy PR, Lev D, Panagiotis GS. *J. Phys. Chem. B* 2002; **106**: 3394.
14. Hannus I, Toth T, Mehn D, Kiricsi I. *J. Mol. Struct.* 2001; **563–564**: 279.
15. Gianotti E, Frache A, Coluccia S, Thomas JM, Maschmeyer T, Marchese L. *J. Mol. Cat. A: Chem.* 2003; **204–205**: 483.
16. Marchese L, Maschmeyer T, Gianotti E, Coluccia S, Thomas JM. *J. Phys. Chem. B.* 1997; **101**: 8836.
17. Chatterjee M, Hayashi H, Siato N. *Micropor. Mesopor. Mater.* 2003; **57**: 143.
18. Shan Z, Jansen JC, Marchese L, Maschmeyer Th. *Micropor. Mesopor. Mater.* 2001; **48**: 181.
19. Blasco T, Corma A, Navarro MT, Pariete P. *J. Catal.* 1995; **156**: 65.
20. Haskouri JE, Cabrera S, Gutierrez M, Beltran-Porter A, Beltran-Porter D, Marcos MD, Amoros P. *Chem. Commun.* 2001; **7**: 1437.
21. Haskouri JE, Zarate DO, Perez-Pla F, Cervilla A, Guillem C, Latorre J, Marcos MD, Beltran A, Beltran D, Amoros P. *New J. Chem.* 2002; **26**: 1093.
22. Frye C, Vicent G, Finzel W. *J. Am. Chem. Soc.* 1971; **93**: 6805.
23. Schacht S, Janicke M, Schuth F. *Micropor. Mesopor. Mater.* 1998; **22**: 485.
24. Liu Z, Sakamoto Y, Ohsuna T, Hiraga K, Terasaki O, Ko CH, Shin HJ, Ryoo R. *Angew. Chem. Int. Ed.* 2000; **39**: 3107.
25. Maria DA, Zhaohou L, Jacek K. *J. Phys. Chem.* 1996; **100**: 2178.
26. Bharat IN, Olanrewaju J, Komarneni S. *Chem. Mater.* 2001; **13**: 552.
27. Rajakovic VN, Mintova S, Senker J, Bein T. *Mater. Sci. Eng. C* 2003; **23**: 817.
28. Raimondi ME, Gianotti E, Marchese L, Martra G, Maschmeyer T, Seddon JM, Coluccia S. *J. Phys. Chem. B* 2000; **104**: 7102.
29. Khushalani D, Ozin GA, Kuperman A. *J. Mater. Chem.* 1999; **9**: 1483.
30. Khushalani D, Ozin GA, Kuperman A. *J. Mater. Chem.* 1999; **9**: 1491.
31. Thanabodeekij N, Gulari E, Wongkasemjit S. *Mater. Chem. Phys.* 2005; accepted for publication.
32. Clague MJ, Bulter A. *J. Am. Chem. Soc.* 1996; **117**: 3475.
33. Clague MJ, Keder NL, Bulter A. *Inorg. Chem.* 1993; **32**: 4754.
34. Sozedjak HS, Bulter A. *Inorg. Chem.* 1990; **29**: 5015.
35. Walker JV, Morey M, Carlsson H, Davidson A, Stucky DG, Bulter A. *J. Am. Chem. Soc.* 1997; **119**: 6921.

